J Fluoresc (2011) 21:1887–1895
DOI 10.1007/s10895-011-0885-4

ORIGINAL PAPER

Spectroscopic Studies on TiO_2 Enhanced Binding of Hypocrellin B with DNA

Ganesan Paramaguru · Rajadurai Vijay Solomon · Ponnambalam Venuvanalingam · Rajalingam Renganathan

Received: 10 December 2010 / Accepted: 23 March 2011 / Published online: 30 March 2011

Abstract The binding of Hypocrellin B-TiO_2 chelate with DNA has been studied by using absorption, steady state fluorescence, cyclic voltammetry, time resolved fluorescence and laser flash photolysis measurements. The experimental results show that the presence of TiO_2 nanoparticles increases the binding of Hypocrellin B with DNA. The groove binding mode is confirmed by spectroscopic and docking studies. Laser flash photolysis studies confirm the presence of electrons in the conduction band of TiO_2 which will produce active oxygen species and results in damage of DNA indicating the potential application of Hypocrellin B-TiO_2 chelate in the field of photodynamic therapy (PDT).

Keywords Hypocrellin B · TiO_2 · DNA · Groove binding · Docking studies

Introduction

Photodynamic therapy (PDT) uses a photosensitizing drug and a light source to activate the applied drug. The result is an activated oxygen molecule that can destroy nearby cells [1]. Precancerous cells and certain types of cancer cells can be treated this way. Hypocrellin B (HB), a perylenequinone photodynamic pigment having strong absorption in the visible region and high photostability was isolated from the natural source Hypocrella bambusae [2]. Scheme 1 shows the chemical structure of HB. The HB have potential photodynamic property for vascular diseases and age related macular degeneration [3]. HB and their derivatives exhibit photosensitized cleavage and damage to DNA in the presence of oxygen [4].

Nowadays semiconductor nanoparticles with unique properties such as large surface area, pore structure have potential applications in optical and electronic properties [5]. Nanoparticles also possess widespread application in biological fields such as clinical diagnostic assays, drug delivery systems and cellular imaging [6, 7]. Nanoparticles are efficiently used as drug carriers since they possess enormous surface area and owing to their sub-micron size they can efficiently be taken up by the cells [8]. The interaction of nanoparticles with various biomolecules has been extensively studied [9, 10]. Recently we have reported the interaction of colloidal TiO_2 with DNA [11]. TiO_2 nanoparticles on photoirradiation generate reactive oxygen species [12] which can damage DNA. Xu et al. have prepared the Hypocrellin B chelate with TiO_2 and its energetics (standard oxidation potential of the excited singlet and triplet states of HB is at −0.68, −0.62 V vs NHE respectively) is thermodynamically favorable to inject charge from its excited state into the conduction band of TiO_2 [13]. Since HB is a good visible photosensitizer with high intersystem crossing quantum yield (ϕ_{ISC}), its interaction with DNA in presence of nanosized TiO_2 (acting as efficient carrier of HB for its better delivery to cancerous part) could reveal useful information in order to tune its application in photodynamic therapy. Hence the combination of nanomaterials with photosensitizers will be a promising pathway in the field of photodynamic therapy. By considering all these advantages we have studied the binding efficiency of Hypocrellin B with DNA in presence of TiO_2 nano particles through absorption, steady state fluorescence, cyclic voltammetry and time resolved fluo-

G. Paramaguru · R. V. Solomon · P. Venuvanalingam · R. Renganathan (✉)
School of Chemistry, Bharathidasan University, Tiruchirappalli 620 024 Tamil Nadu, India
e-mail: rrengas@gmail.com

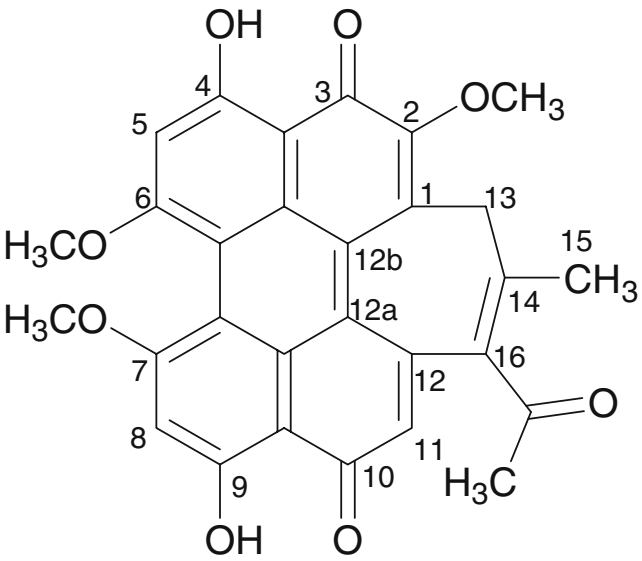

Scheme 1 Structure of Hypocrellin B

rescence measurements. The mode of interaction is found to be groove binding which is further supported by docking studies. The formation of conduction band electrons is confirmed through laser flash photolysis which can reduce dioxide to superoxide radicals.

Materials and Methods

Materials

Hypocrellin B was purchased from LKT Laboratories, USA. Double stranded Calf thymus-deoxyribonucleic acid and titanium (IV) 2-propoxide were purchased from Aldrich (Bangalore, India). The stock solution of DNA was prepared by dissolving an appropriate amount of DNA in phosphate buffer. The concentration of the DNA stock solution (7×10^{-4} M) was determined from the UV absorption spectrum at 260 nm using the molar absorption coefficient ε_{260}=6600 M^{-1} cm^{-1}. The purity of the DNA was checked by monitoring the ratio of the absorbance at 260 nm to that at 280 nm. The resulting ratio, $A_{260}/A_{280}>$ 1.8, indicates that DNA was sufficiently free from protein [14]. Due to the low solubility of Hypocrellin B in water, the solution (1×10^{-3} M) was prepared by adding small amounts of DMSO solution to double distilled water [15].

Preparation of Colloidal TiO_2 Nanoparticles

The colloidal TiO_2 nanoparticle was prepared by the hydrolysis of titanium (IV) 2-propoxide, based on the literature procedure [16]. Typically, titanium (IV) 2-propoxide (15 μl) in 2-propanol (150 μl) was injected into 50 ml of water using syringe (Prior to experiment, pH of water adjusted to 1.5 using 1 M $HClO_4$ solution) with constant stirring under nitrogen atmosphere (for 8 h) resulting in a 1×10^{-3} M titania stock solution. No stabilizing agent was used during the hydrolysis process. The colloidal suspensions of TiO_2 prepared by this method were stable for 3–5 days. Fresh colloidal TiO_2 dispersed in water was prepared before each set of experiments. The stock suspension was diluted with water to obtain the desired concentrations of TiO_2. No attempts were made to exclude the traces of 2-propanol present in the colloidal TiO_2 nanoparticles and it was reported that the presence of 2-propanol did not affect the photochemical measurements [17]. The absorption of the colloidal TiO_2 in water is observed at 330 nm. The diameter of the particles determined from the relationship between band gap shift (ΔE_g) and radius (R) of quantum-size particles [11] is about 4.1 nm.

Steady-state Measurements

The fluorescence quenching measurements were carried out with JASCO FP-6500 spectrofluorimeter. The excitation and emission wavelength of Hypocrellin-TiO_2 chelate are 460 and 610 nm respectively. The slit widths 20 nm and scan rate (500 nm/min) for both excitation and emission were maintained constant for all the measurements. The samples were purged with pure nitrogen before measurements. Quartz cells (4×1×1 cm) with high vacuum Teflon stopcocks were used for measurements. Absorption spectral measurements were recorded using JASCO V630 UV–visible spectrophotometer.

Electrochemical Measurements

The cyclic voltammetry measurements were carried out with CHI 650 C, USA, CH measurements. Potassium chloride (0.1 M) is used as supporting electrolyte. The experimental setup consisted of a platinum working electrode, a glassy carbon counter electrode and a silver reference electrode. All samples were deaerated by bubbling with pure nitrogen gas for ca. 5 min at room temperature.

Docking Studies

The docking analysis has been carried out using AutoDock 4.0 package. The crystal structure of B-DNA was obtained from Protein Data Bank (PDB code 453D) [18]. Polar hydrogen atoms with Gasteiger charges were added and water molecules were removed. The Hypocrellin-B structure was optimized at B3LYP/6-31 G* level using G03W program [19]. The Lamarckian Genetic Algorithm (LGA)

was used with default parameters during the docking process [20]. This algorithm includes terms for changes in energy due to van der Waals interaction, hydrogen bonding and electrostatic forces, as well as ligand torsion and desolvation. Auto Dock reports a docked energy that includes a solvation-free energy term and intermolecular interaction energy of the ligand.

Time Resolved Fluorescence Measurements

Fluorescence lifetime measurements were carried out in a picosecond time correlated single photon counting (TCSPC) spectrometer. The excitation source is the tunable Ti-sapphire laser (Tsunami, Spectra Physics, USA). The fluorescence decay was analyzed by using the software provided by IBH (DAS-6).

Laser Flash Photolysis

The Nd-YAG laser source produces nanosecond pulses (8 ns) of 500 nm light and energy of the laser pulse was around 150 mJ. Dichroic mirrors were used to separate the third harmonic from the second harmonic and the fundamental output of the Nd-YAG laser. The monitoring source was a 150W pulsed xenon lamp which was focused on the sample at 90° to the incident laser beam. The beam emerging through the sample was focused onto a Czerny-Turner monochromator using a pair of lenses. The detection was carried out using a Hamamatsu R-928 photomultiplier tube. The transient signals were captured with an Agilent infiniium digital storage oscilloscope interfaced to a computer.

Results and Discussion

Absorption Studies

Figure 1A shows the absorption spectra of HB and HBT. HB shows absorption at 460 nm. In presence of TiO_2 the absorption maxima was red shifted to 474 nm which indicates a chelate formation (HBT) as previously reported [21, 22]. Figure 1B shows the fluorescence excitation spectrum of HB and HBT in water. The presence of TiO_2 nanoparticles changes the excitation spectra of HB which further confirms the formation of ground state complex between the HB and TiO_2 nanoparticles.

Generally intercalation of drug molecules to DNA usually results in decrease in intensity (hypochromism) in the absorption behavior with substantial red shift [23]. Figure 2A shows the absorption spectra of HBT in the absence and presence of DNA. HBT shows absorption at 474 nm. On increasing the concentration of DNA the

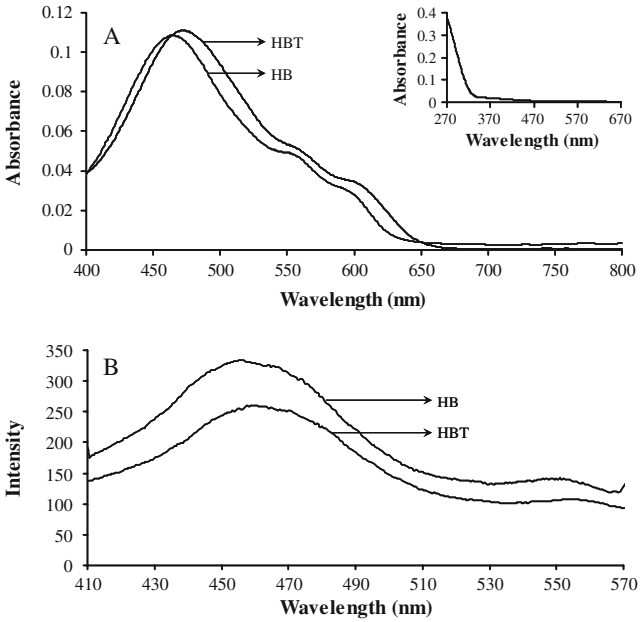

Fig. 1 **A** Absorption spectrum of Hypocrellin B (HB) and Hypocrellin B-TiO_2 (HBT) in water. The inset is the absorption spectrum of colloidal TiO_2 nanoparticles in water. **B** Excitation spectrum of HB and HBT in water

absorption band at 474 nm shifted to longer wavelength (484 nm) and also shows a significant hyperchromism suggesting that the presence of a strong ground state

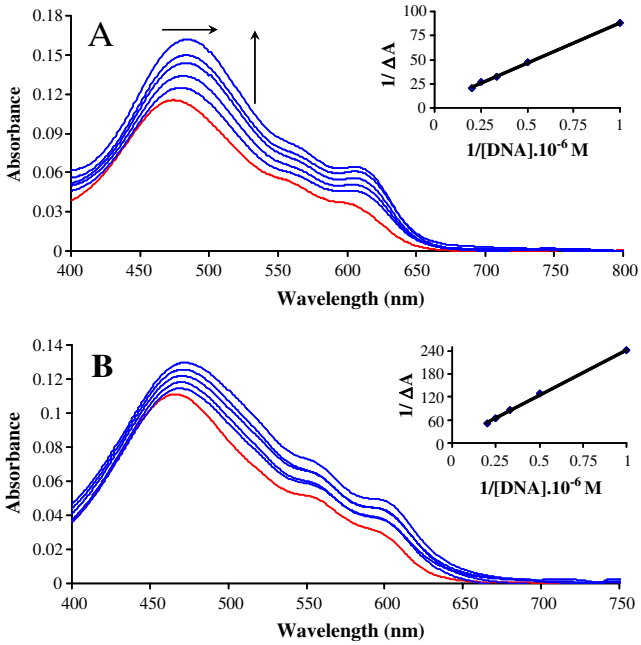

Fig. 2 **A** Absorption spectrum of HBT (1×10^{-6} M; *red color*) in the presence (*blue color*) of DNA ($0–5\times10^{-6}$ M) in water. The inset is the linear dependence of $1/\Delta A$ on the reciprocal concentration of DNA. **B** Absorption spectrum of HB (1×10^{-6} M; *red color*) in the presence (*blue color*) of DNA ($0–5\times10^{-6}$ M) in water. The inset is the linear dependence of $1/\Delta A$ on the reciprocal concentration of DNA

complex between HBT and DNA which is different from the general intercalation binding. Similar type of hyperchromism in presence of DNA has been reported [24]. Based on the reports the spectral changes can be rationalized in terms of groove binding [24, 25]. The absorbance behavior of HB with DNA is studied to understand the influence of TiO_2 in binding efficiency of HBT with DNA. Figure 2B shows the effect of increasing concentration of DNA on the absorption spectra of Hypocrellin B. While increasing the concentration of DNA a slight hyperchromism and red shift is observed but the observed difference is much less when compared to the HBT chelate system. Thus it is apparent from absorbance study that the HB and HBT form a ground state complex with DNA. Figure 3 shows the difference absorption spectra of HBT in the presence of DNA in water. The appearance of isobestic point on increasing the concentration of DNA supports the formation of complex formation between HBT and DNA.

The binding strength of HBT and HB with DNA was calculated by considering a simple equilibrium system where the equilibrium constant for complex formation can be estimated from changes in absorbance using Benesi Hildebrand Eq. 1 [26].

$$\frac{1}{\Delta A} = \frac{1}{(A_c - A_0)} + \frac{1}{K_b(A_c - A_0)[DNA]} \quad (1)$$

where ΔA is the change in absorbance at a fixed wavelength, A_0 and A_c are the absorbance of free sensitizer and the complex respectively. For the complex formation a linear relationship will be obtained between $1/\Delta A$ and the reciprocal concentration of [DNA]. The ratio of the intercept $1/(A_c - A_0)$ to the slope $1/K_b(A_c - A_0)$ gives the binding constant for complex formation and the values are listed in Table 1. The binding constant value of HBT is found higher than that of HB. The results clearly indicate that the formation of TiO_2 chelate could increase the binding affinity of HB with DNA. The different binding behavior in the presence of TiO_2 chelate with DNA may be attributed to the large surface area on nano TiO_2 which provides efficient binding with DNA.

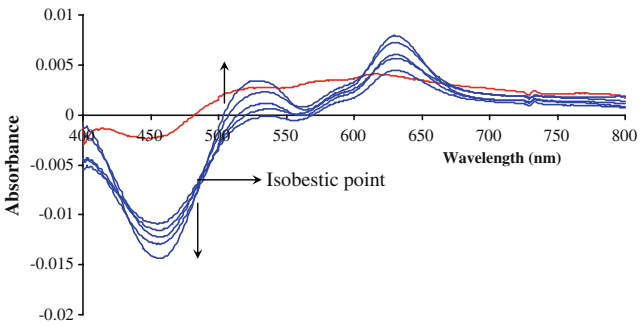

Fig. 3 Difference absorption spectra of the HBT (*red color*) in presence of various concentration of DNA (*blue color*). *Arrow* indicates the change in addition of $0–5\times10^{-6}$ M DNA respectively

Electrochemical Measurements

Electrochemical studies were carried out to support the role of TiO_2 nanoparticles in the binding of HB with DNA. Figure 4 shows the cyclic voltammogram (CV) of HB, HB with DNA and HB with DNA in the presence of TiO_2 nanoparticles. Considerable decrease in peak current is observed for HB in the presence of DNA. In the presence of TiO_2 nanoparticles the CV of HB with DNA shows a shift in peak potentials along with bigger decrease in peak current. Similar type of change in peak currents in presence of nanoparticles has been reported [27]. On the basis of these results it is evident that the presence of TiO_2 nanoparticles enhances the binding affinity of HB with DNA which supports the results obtained from absorption measurements.

Effect of Ionic Strength

The change of ionic strength is an efficient method for distinguishing the binding modes between small molecules and DNA. Figure 5 shows the effect of sodium chloride on the fluorescence spectrum of HBT-DNA system. If the binding of HBT with DNA is due to electrostatic interactions then the negative charges of the DNA phosphatic back bone will be partly neutralized by Na^+ ions. Hence electrostatic binding will result in increase in the intensity of fluorescence with increase in Na^+ concentration. In our case, there is no increase in fluorescence intensity while increasing the concentration of Na^+. Hence the results suggest that the binding is not electrostatic in nature. But a decrease in fluorescence intensity is observed, this may be due to the existence of Na^+ which makes the double helix structure of DNA gather together longitudinally and makes the way for groove binding [28]. The results from the absorption and ionic strength measurements suggest the interaction between HBT and DNA occurs through groove binding mode.

Molecular Docking Investigations

Docking analysis has been carried out to gain further insights into the binding nature of HB with DNA. The resultant docked conformation of the HB bound DNA is given in Fig. 6. The results reveal that the HB fits well within the minor groove of DNA and the binding site covers 3 base pairs long, involving A-T residues. A similar type of minor groove binding has been reported for different ligand-DNA interactions [29, 30].

Table 1 Stern–Volmer constants (K_{SV}), Quenching rate constants (k_q), Binding constant (K_b) calculated for the HB and HBT with DNA

	$K_{SV}/(M^{-1})$	$k_q/(M^{-1}s^{-1})$	$K_b/(M^{-1})$	
			Absorbance	Fluorescence
HB:DNA	7.03×10^4	4.15×10^{13}	2.64×10^4	4.40×10^4
HBT:DNA	4.15×10^5	3.09×10^{14}	5.88×10^5	4.84×10^5

Earlier reports suggested that the interactions of C-2 carbonyl oxygen of thymine and N3 nitrogen of adenine with the ligand are essential for the minor groove binding [31] which exactly correlates with our results. Our calculations show that the 7th position $-OCH_3$ of HB situated at a distance of 1.84 Å from C-2 carbonyl oxygen of thymine (T) and at the same time, the 9th position −OH of HB is at a distance of 3.1 Å from N3 of adenine which substantiate the minor groove binding nature.

Fluorescence Quenching Studies

Fluorescence quenching measurements have been widely used to study the interaction of various drugs with biological molecules [29, 32]. This method helps to understand DNA binding mechanisms with other molecules and provide clues to the nature of the binding. In principle, molecules that are either free or bound on the surface of DNA are easily accessible for the quencher while those which are intercalated are protected from the quencher.

The interaction of HBT with DNA was studied by fluorescence measurement at room temperature. Fluorescence spectra were recorded in the range of 570–750 nm upon excitation at 460 nm. DNA is transparent at the 460 nm excitation wavelength. Figure 7A shows the effect of increasing concentration of DNA on the fluorescence emission spectrum of HBT. It is observed that the fluorescence emission band of HBT is quenched with increasing concentration of DNA. The HB-DNA system in the absence of TiO_2 also gave a similar type of fluorescence behavior (Fig. 7B). The fluorescence quenching can be described by Stern-Volmer relation:

$$I_0/I = 1 + K_{SV}[Q] = 1 + k_q\tau_0[Q] \quad (2)$$

where, I_0 and I are the fluorescence intensities of the fluorophore in the absence and presence of quencher, K_{SV} is the Stern-Volmer constant, k_q is the bimolecular quenching rate constant, τ_0 is the excited state lifetime of fluorophore in the absence of quencher and [Q] is the quencher concentration. A plot of I_0/I against [DNA] results in a linear plot. The K_{sv} value is obtained from the slope and the values are listed in the Table 1. Since the lifetime of HBT is in the order of 10^{-9} s, the calculated bimolecular quenching rate constant (k_q) using $K_{sv}=k_q\tau_0$ was found to be higher than the maximum collisional quenching (k_q) of various kind of quenchers to biopolymers (2.0×10^{10} $M^{-1}s^{-1}$). Hence the fluorescence quenching results from complex formation between DNA and HB-TiO_2 chelate and not due to dynamic nature [33]. The fluorescence behavior of HB-DNA system in the absence of TiO_2 also shows the static type of behavior.

In general, time resolved measurement is the most definitive method for differentiating static and dynamic quenching. Figure 8 shows the fluorescence decay curve of HBT in the absence and presence of DNA. In the presence of DNA there is no change in the fluorescence lifetime of HB. This observation shows that quenching follows static mechanism. Static quenching does not decrease the lifetime

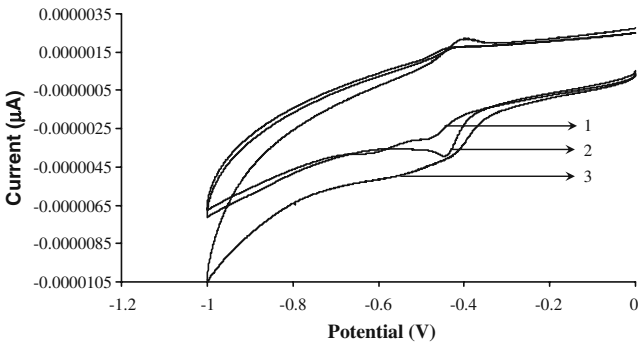

Fig. 4 Cyclic voltammogram of (*1*) HB (1×10^{-5} M), (*2*) HB (1×10^{-5} M) in presence of DNA (1×10^{-5} M), (*3*) HB (1×10^{-5} M) in presence of DNA (1×10^{-5} M) and TiO_2 nanoparticles (1×10^{-5} M)

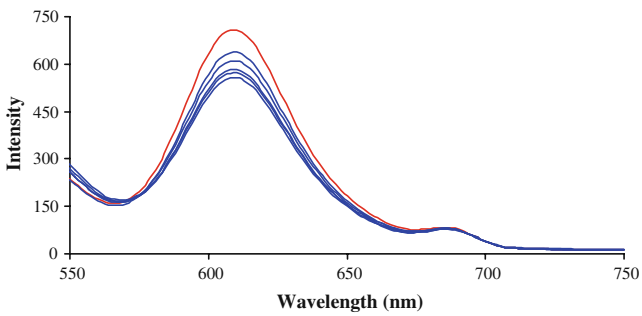

Fig. 5 Fluorescence Quenching of HBT (1×10^{-6} M; λ_{ex}=460 nm; λ_{em}=610 nm) in the absence (*red color*) and presence (*blue color*) of various concentration of NaCl, [NaCl] = 0–5×10^{-6} M

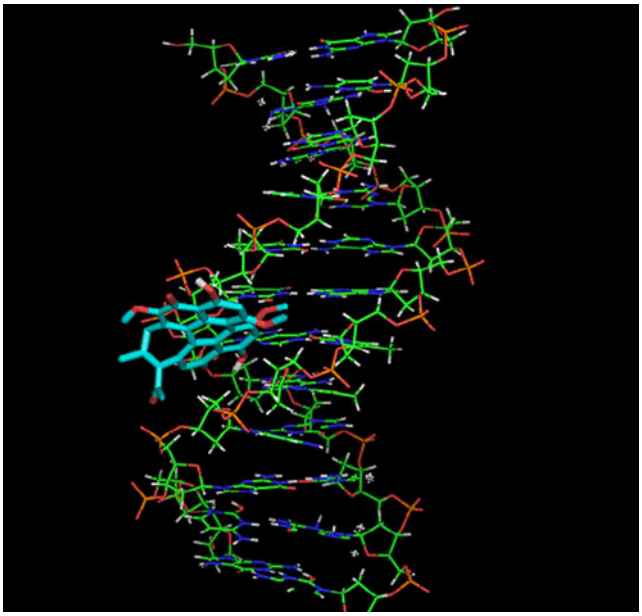

Fig. 6 Positioning of Hypocrellin-B in the minor groove of the DNA obtained from docking studies

because only the fluorescent molecules are observed, and the uncomplexed fluorophores have the unquenched lifetime [34]. Static quenching arises due to the formation of

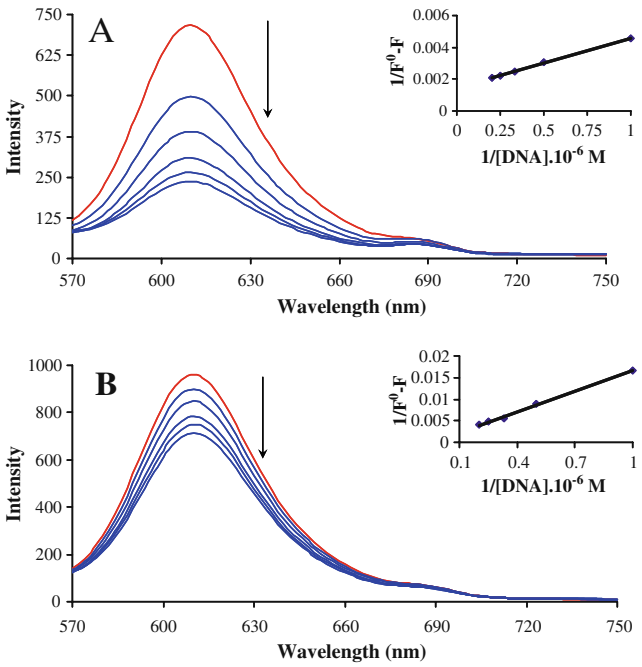

Fig. 7 **A** Fluorescence Quenching of HBT (1×10^{-6} M; λ_{ex}=460 nm; λ_{em}=610 nm) in the absence (*red color*) and presence (*blue color*) of various concentration of DNA, [DNA] = 0–5×10^{-6} M. The inset is the straight line dependence of $1/(F^0–F)$ on the reciprocal concentration of DNA. **B** Fluorescence Quenching of HB (1×10^{-6} M; λ_{ex}=460 nm; λ_{em}= 610 nm) in the absence (*red color*) and presence (*blue color*) of various concentration of DNA, [DNA] = 0–5×10^{-6} M. The inset is the straight line dependence of $1/(F^0–F)$ on the reciprocal concentration of DNA

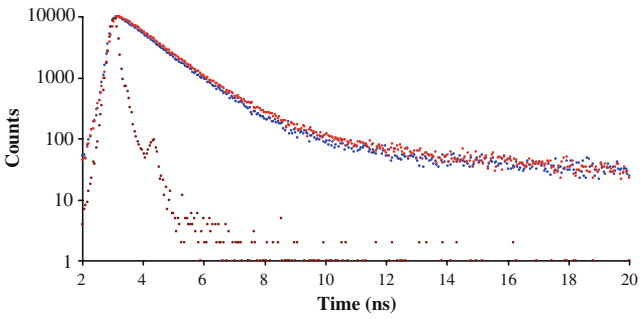

Fig. 8 Fluorescence lifetime decay curves of (*i*) Instrument response curve (Brown colour decay). (*ii*) HBT (Red colour decay), (*iii*) HBT in the presence of DNA (Blue colour decay)

complex between fluorophore and the quencher. Hence from the fluorescence measurements the binding affinities of HBT to DNA were calculated from the following Eq. 3.

$$\frac{1}{(F^0-F)}=\frac{1}{(F^0-F')}+\frac{1}{K_b(F^0-F')[DNA]} \quad (3)$$

where F^0 is the fluorescence intensity of free HBT, F′ is the fluorescence intensity of HBT in the presence of DNA and F is the observed fluorescence intensity at its maximum. A plot of $1/(F^0\text{-}F)$ Versus 1/[DNA] gives a straight line and from the slope the binding constant (K_b) was calculated. The K_b for HB-DNA system was also

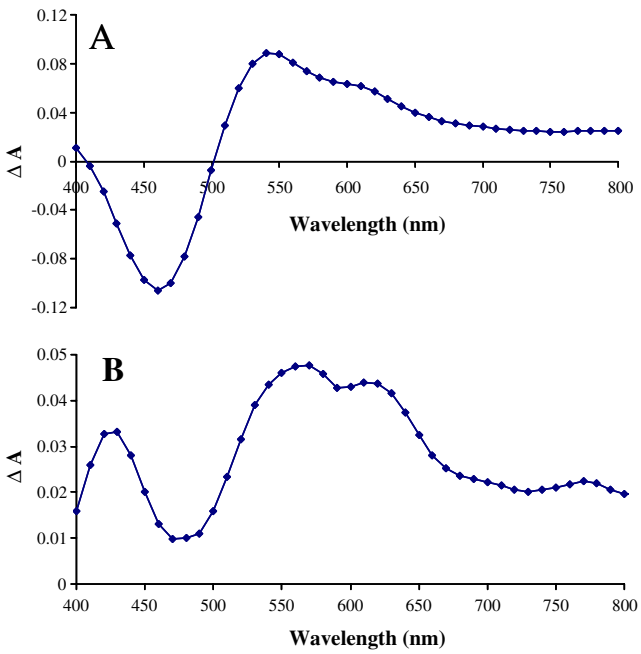

Fig. 9 **A** Transient difference absorption spectra of HB recorded at 4 μs after the laser flash at 500 nm. **B** Transient difference absorption spectra of HBT-DNA recorded at 4 μs after the laser flash at 500 nm

Scheme 2 Formation of reactive oxygen species

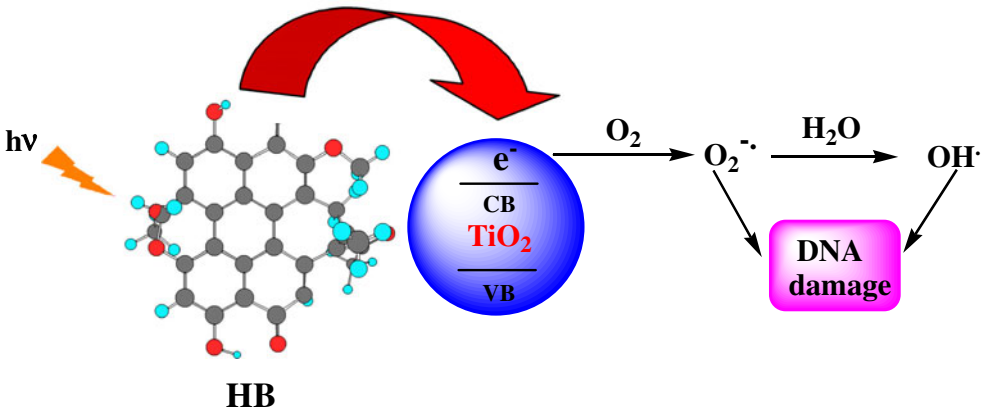

calculated. The K_b of both HBT-DNA and HB-DNA are listed in Table 1. K_{sv} and K_b of HBT-DNA obtained from both absorption and fluorescence measurement was higher than that of HB-DNA. The larger value indicates a stronger interaction between the HBT and DNA. The fluorescence results also support that the HBT system would enhance the binding affinity with DNA which is a basic requirement in PDT.

Laser Flash Photolysis

The excited state HB may undergo energy or electron transfer with TiO_2 which results in the formation of active oxygen species ($^1O_2$ and $O_2^{\cdot-}$) [35]. Zhang M. H et al. have reported that the decrease in fluorescence intensity of HB attributed to electron transfer to the conduction band of TiO_2 [21, 22] which results in the formation of cation radical ($HB^{\cdot+}$) of HB and the conduction band electron of TiO_2. Hence the electron in the conduction band of TiO_2 is involved in the formation of superoxide radicals ($O_2^{\cdot-}$).

Laser flash photolysis has been widely used to study the excited state electron transfer reactions. Nanosecond laser flash photolysis experiments were carried out using 500 nm laser pulse as the excitation source. Figure 9A shows the transient absorption spectra of HB in aqueous medium and the absorption band appears at 540 nm is similar to the earlier reported T-T absorption of HB in n-hexane [36]. Bleaching in the region of 460 nm corresponds to the HB ground-state bands. The transient absorption spectra of HBT-DNA system is shown in Fig. 9B. Significant differences were observed for HBT DNA system when compared to HB system. A new peak appeared at around 570 nm which was ascribed to the cation radical of $HB^{\cdot+}$ [35] and a peak above 750 nm extending over visible region to the near IR region is due to conduction band electron of TiO_2 which matched well with previously reported observations [36]. These observations confirm the presence of an electron in the conduction band of TiO_2 which undergoes rapid reoxidation to produce the superoxide radical anion in the presence of oxygen and results in DNA damage (Scheme 2).

Conclusions

The binding of the biologically important Hypocrellin B in presence of TiO_2 with DNA has been examined through various spectroscopic measurements. Absorption and difference absorption studies indicate the formation of ground state complex between HBT and DNA. Fluorescence quenching follows static mechanism and groove type binding mode is confirmed by docking studies. The presence of TiO_2 nanoparticles enhance the binding strength of HB with DNA which was confirmed from the binding constant values calculated from absorption and steady state measurements. Electrochemical studies further support the role of TiO_2 nanoparticles in binding of HB with DNA. Laser flash photolysis confirms the presence of conduction band electron of TiO_2 in HBT-DNA system which further forms superoxide radicals to damage DNA. All these results put forward that the PDT behavior of HB with DNA will be enhanced in the presence of TiO_2 which implies its potential application for future designing of more efficient PDT drugs.

Acknowledgements R. R and G. P thank CSIR (Ref. No. 01(2217)/08/EMR-II, dt. 06/05/2008) for the Project and Fellowship respectively. P. V thanks the CSIR, India, for their financial support in the form of a research grant (Ref. No. 02(2158)/07/EMR-II). P. V and R. VS thank the UGC, INDIA for the financial support through Maulana Azad National Fellowship (Ref. No. F.40-17(C/M)/2009(SA-III/MANF). Authors also thank UGC/DST-FIST for UV–VIS and Fluorescence facilities in the School of Chemistry, Bharathidasan University. We are thankful to Prof. P. Ramamurthy, NCUFP, University of Madras, Chennai for time resolved measurements and Laser flash photolysis. We are thankful to Dr. S. Anandan, National Institute of Technology, Trichy for cyclic voltammetry measurements.

References

1. Ackroyd R, Kelty C, Brown N, Reed M (2001) The history of photodetection and photodynamic therapy. Photochem Photobiol 74:656–669
2. Diwu Z, Lown JW (1992) Photosensitization by anticancer agents 12. Perylene quinonoid pigments, a novel type of singlet oxygen sensitizer. J Photochem Photobiol A Chem 64:273–287
3. Zhou J, Liu J, Xia S, Wang X, Zhang B (2005) Effect of chelation to lanthanum ions on the photodynamic properties of Hypocrellin A. J Phys Chem B 109:19529–19535
4. Zhang J, Cao EH, Li JF, Zhang TC, Ma WJ (1998) Photodynamic effects of hypocrellin A on three human malignant cell lines by inducing apoptotic cell death. J PhotochemPhotobiol B Biol 43:106–111
5. Artemyev MV, Woggon U, Wannemacher R, Jaschinski H, Langbein W (2001) Light trapped in a photonic dot: microspheres act as a cavity for quantum dot emission. Nano Lett 1:309–314
6. Bruchez M, Moronne M, Gin P, Weiss S, Alivisatos AP (1998) Semiconductor nanocrystals as fluorescent biological labels. Science 281:2013–2016
7. Wu X, Liu H, Liu J, Haley K, Treadway J, Larson J, Ge N, Peals F, Bruchez M (2003) Immunofluorescent labeling of cancer marker Her2 and other cellular targets with semiconductor quantum dots. Nat Biotechnol 21:41–46
8. Wiseman A (1985) Handbook of enzyme biotechnology. Horwood Chichester
9. Kathiravan A, Paramaguru G, Renganathan R (2009) Study on the binding of colloidal zinc oxide nanoparticles with bovine serum albumin. J Mol Struct 934:129–137
10. Kathiravan A, Renganathan R, Anandan S (2009) Interaction of colloidal $AgTiO_2$ nanoparticles with bovine serum albumin. Polyhedron 28:157–161
11. Kathiravan A, Renganathan R (2009) Photoinduced interactions between colloidal TiO_2 nanoparticles and calf thymus-DNA. Polyhedron 28:1374–1378
12. Tachikawa T, Majima T (2009) Single-molecule fluorescence imaging of TiO_2 photocatalytic reactions. Langmuir 25:7791–7802
13. Ma JN, Jiang LJ, Zhang MH, Yu Q (1989) Delayed fluorescence of hypocrellins and absorption spectra of isomers. Chin Sci Bull 34:1442–1448
14. Marmur J (1961) A procedure for the isolation of deoxyribonucleic acid from micro-organisms. J Mol Biol 3:208–218
15. Zhou J, Wu X, Gu X, Zhou L, Song K, Wei S, Feng Y, Shen J (2009) Spectroscopic studies on the interaction of hypocrellin A and haemoglobin. Spectrochim Acta 72:151–155
16. Kamat PV (1985) Photoelectrochemistry in particulate systems. 3. Phototransformations in the colloidal titania-thiocyanate system. Langmuir 1:608–611
17. Kamat PV, Chauvet JP, Fessenden RW (1986) Photoelectrochemistry in particulate systems. 4. Photosensitization of a titanium dioxide semiconductor with a chlorophyll analog. J Phys Chem 90:1389–1394
18. Berman HM, Westbrook J, Feng Z, Gilliland G, Bhat TN, Weissig H, Shindyalov IN, Bourne PE (2000) The protein data bank. Nucleic Acids Res 28:235–242
19. Frisch MJ, Trucks GW, Schlegel HB, Scuseria GE, Robb MA, Cheeseman JR, Montgomery JA, Vreven T, Kudin KN, Burant JC, Millam JM, Iyengar SS, Tomasi J, Barone V, Mennucci B, Cossi M, Scalmani G, Rega N, Petersson GA, Nakatsuji H, Hada M, Ehara M, Toyota K, Fukuda R, Hasegawa J, Ishida M, Nakajima T, Honda Y, Kitao O, Nakai H, Klene M, Li X, Knox JE, Hratchian HP, Cross JB, Bakken V, Adamo C, Jaramillo J, Gomperts R, Stratmann RE, Yazyev O, Austin A, Cammi R, Pomelli C, Ochterski JW, Ayala PY, Morokuma K, Voth GA, Salvador P, Dannenberg JJ, Zakrzewski VG, Dapprich S, Daniels AD, Strain MC, Farkas O, Malick DK, Rabuck AD, Raghavachari K, Foresman JB, Ortiz JV, Cui Q, Baboul AG, Clifford S, Cioslowski J, Stefanov BB, Liu G, Liashenko A, Piskorz P, Komaromi I, Martin RL, Fox DJ, Keith T, Al-Laham MA, Peng CY, Nanayakkara A, Challacombe M, Gill PMW, Johnson B, Chen W, Wong MW, Gonzalez C, Pople JA (2004) Gaussian 03, Revision C.02. Gaussian, Inc, Wallingford
20. Morris GM, Goodsell DS, Huey R, Olson AJ (1996) Distributed automated docking of flexible ligands to proteins: parallel applications of AutoDock 2.4. J Comput Aided Mol Des 10:293–304
21. Wu T, Xu S, Shen J, Chen S, Zhang M, Shen T (2000) Photosensitization of TiO_2 colloid by hypocrellin B in ethanol. J Photochem Photobiol A Chem 137:191–196
22. Rajh T, Chen LX, Lukas K, Liu T, Thurnauer MC, Tiede DM (2002) Surface restructuring of nanoparticles: an efficient route for ligand-metal oxide crosstalk. J Phys Chem B 106:10543–10552
23. Kelly JM, Tossi AB, McConnell DJ, OhUigin C (1985) A study of the interactions of some polypyridylruthenium(II) complexes with DNA using fluorescence spectroscopy, topoisomerisation and thermal denaturation. Nucleic Acids Res 13:6017–6034
24. Liu Z, Jiang M, Li Y, Wu Z, Yang J (2009) One-dimensional copper(II) polymer with bridging μ-trans-oxamidate and thiocyanate ligands: synthesis, crystal structure and DNA binding studies. Inorg Chim Acta 362:1253–1259
25. Bazzicalupi C, Bencini A, Bianchi A, Biver T, Boggioni A, Bonacchi S, Danesi A, Giorgi C, Gratteri P, Ingra AM, Secco F, Sissi C, Valtancoli B, Venturini M (2008) DNA binding by a new metallointercalator that contains a proflavine group bearing a hanging chelating unit. Chem Eur J 14:184–196
26. Benesi HA, Hildebrand JH (1949) A spectrophotometric investigation of the interaction of iodine with aromatic hydrocarbons. J Am Chem Soc 71:2703–2707
27. Wang X, Zhang R, Wu C, Dai Y, Song M, Gutmann S, Gao F, Lv G, Li J, Li X, Guan Z, Fu D, Chen B (2007) The application of Fe_3O_4 nanoparticles in cancer research: a new strategy to inhibit drug resistance. J Biomed Mater Res A 80A:852–860
28. Bi S, Qiao C, Song D, Tian Y, Gao D, Sun Y, Zhang H (2006) Study of interactions of flavonoids with DNA using acridine orange as a fluorescence probe. Sens Actuators B 119:199–208
29. Saquib Q, Al-Khedhairy AA, Alarifi SA, Dutta S, Dasgupta S, Musarrat J (2010) Methyl thiophanate as a DNA minor groove binder produces MT–Cu(II)–DNA ternary complex preferably with AT rich region for initiation of DNA damage. Int J Biol Macromol 47:68–75
30. Bera R, Sahoo BK, Ghosh S, Dasgupta S (2008) Studies on the interaction of isoxazolcurcumin with calf thymus DNA. Int J Biol Macromol 42:14–21
31. Zsila F, Bikádi Z, Simonyi M (2004) Circular dichroism spectroscopic studies reveal pH dependent binding of curcumin in the minor groove of natural and synthetic nucleic acids. Org Biomol Chem 2:2902–2910
32. Das S, Kumar GS (2008) Molecular aspects on the interaction of phenosafranine to deoxyribonucleic acid: model for intercalative drug–DNA binding. J Mol Struct 872:56–63

33. Sun W, Du Y, Chen J, Kou J, Yu B (2009) Interaction between titanium dioxide nanoparticles and human serum albumin revealed by fluorescence spectroscopy in the absence of photoactivation. J Lumin 129:778–783
34. Lakowicz R (2006) Principles of fluorescence spectroscopy, 3rd edn. Springer Science + Business Media, New York, p 281, Chapter 8
35. Xu S, Shen J, Chen S, Zhang M, Shen T (2002) Active oxygen species ($^1O_2$, O^{2-}) generation in the system of TiO_2 colloid sensitized by hypocrellin B. J Photochem Photobiol B 67:64–70
36. Weng M, Zhang M, Wang W, Shen T (1997) Investigation of triplet states and radical anions produced by laser photoexcitation of hypocrellins. J Chem Soc Faraday Trans 93:3491–3495